

Nonresonant Excess Photon Detachment of Negative Hydrogen Ions

Xin Miao Zhao,¹ M. S. Gulley,² H. C. Bryant,² Charlie E. M. Strauss,¹ David J. Funk,¹ A. Stintz,² D. C. Rislove,²
G. A. Kyrala,¹ W. B. Ingalls,¹ and W. A. Miller²

¹Los Alamos National Laboratory, P.O. Box 1663, Los Alamos, New Mexico 87545

²Department of Physics and Astronomy, University of New Mexico, Albuquerque, New Mexico 87131

(Received 22 August 1996)

We report the first observation of nonresonant excess photon absorption (for ionization as well as detachment) in competition with the single photon process. A 35 keV negative hydrogen ion beam is irradiated with focused Nd:YAG laser pulses; the 1.165 eV photon energy exceeds the electron binding energy by 0.41 eV. The time of flight spectrum of detached electrons exhibits the absorption of one and two photons. The detached electrons exit with a *P* wave angular distribution for the one-photon detachment and primarily a *D* wave for the two photon excess photon detachment. [S0031-9007(97)02313-2]

PACS numbers: 32.80.Gc, 32.80.Wr

As is well known, multiphoton ionization occurs when an atom absorbs multiple photons and ejects an electron. Furthermore, atoms and ions can absorb photons beyond the minimum number necessary to eject an electron. This process, whose signature is an electron bearing excess energy from absorbing more than the minimum number of photons, is known as above threshold ionization (ATI) [1] in atoms, and as excess photon detachment (EPD) or, equivalently, above threshold detachment (ATD) [2–4] in negative ions.

Early observations of EPD used photons with energies well below the ion binding energy [2–4]. Studies using photons above the binding energy are hampered by the strong one-photon detachment. Previously, the absorption of a second photon in this regime was observed only when enhanced by an intermediate “window” resonance [5] or final state resonance [6]. This work describes the first observation of EPD with photon energy above the binding energy without resonance enhancement in the negative hydrogen ion, H^- .

H^- is a fundamentally interesting system for the study of EPD since it is the simplest bound three-body Coulombic system, has no singly excited Rydberg levels, and, consequently, differs from neutral atoms in electron photo-ejection dynamics. There are no stepping stones (either bound states nor resonance in the region under consideration), and the long range final state field is that of an induced dipole rather than that of a monopole. The electron has a binding energy of 0.7542 eV [7], and the broadly peaked absorption continuum is featureless below the onset of detachment resonances near 11 eV. Previous multiphoton detachment measurements on H^- with laser energies below the binding energy were not sensitive to the EPD process [8]. Prior to this work, EPD in H^- had been reported only in resonance with the lowest lying (1D) two-photon resonance near 10.87 eV [6].

We observed nonresonant EPD in H^- with the absorption of two photons of energy 1.165 eV. This

regime is particularly interesting because the one- and two-photon energies are not near any intermediate or final state resonances. The photon energy lies near the maximum [9] of the single photon absorption continuum, well beyond the threshold. The principal experimental obstacle is that single photon detachment depletes the ions before they can reach the intense field region where nonlinear processes occur appreciably. Nevertheless, we resolved two-photon EPD photoelectrons in the energy spectrum resulting from a fast, high current, ion source [10] directed through a focused laser beam. An alternative approach to quickly raise the photon field intensity would be to use a picosecond laser [11] with a slow moving H^- beam.

As diagrammed in Fig. 1, an ion beam crosses a laser beam at a right angle, and the kinetic energy distribution of the ejected electrons is recorded. In the ion beam rest frame, the detached electrons acquire a kinetic energy $T_e = Nh\nu - E_b$, where N is the number of photons absorbed, $h\nu$ is the photon energy, and E_b is the electron binding energy. Although the electrons are ejected in

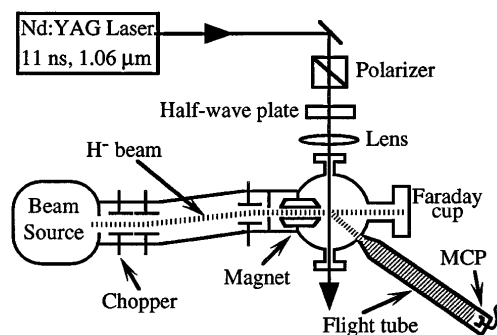


FIG. 1. The negative hydrogen ion beam passes through a cylindrically focused laser beam. A half-wave plate rotates the polarization angle. The kinetic energy spectrum of the detached electrons is determined from the time of flight through the magnetic solenoid bottle to the MCP.

all directions, a magnetic field bends and collimates them along the time-of-flight (TOF) tube axis so that, in the laboratory frame, the electron kinetic energy is approximately

$$T_{\text{lab}} = T_0 + T_e + 2\sqrt{T_0 T_e} \cos \theta, \quad (1)$$

where $T_0 = mv_0^2/2$, with m , the electron mass, v_0 , the ion beam velocity, and θ , the angle at which the electron is ejected with respect to the ion beam axis [12]. If the ion is initially with zero angular momentum, as it is in our experiment (H^- in its only bound state, $1S^e$), and the laser is linearly polarized at an angle Φ with respect to the ion beam axis, one can derive an expression for the differential arrival time cross section after a flight distance d in the TOF tube [6,13],

$$\frac{d\sigma}{dt} = \frac{1}{\sqrt{T_e T_0}} \frac{md^2}{t^3} \frac{\sigma}{4} f(\theta, \Phi), \quad (2)$$

and

$$f(\theta, \Phi) = 1 + \sum_{k=1}^N \beta_{2k} P_{2k}(\cos \theta) P_{2k}(\cos \Phi), \quad (3)$$

where $P_{2k}()$ are Legendre polynomials. Equation (3) arises from the addition theorem of Legendre polynomials, averaging over the azimuthal angle. We seek to determine the anisotropy of the electron angular distribution given by the β_{2k} coefficients.

The experimental setup is essentially the same as in Ref. [6] with changes to the laser source. The ion source provides an H^- beam with 8 μA instantaneous current in pulses of 100 ns duration at 5 Hz and an ion energy of 35 keV. Since transient spikes and hot spots in multimode laser beams may impede reliable modeling of multiphoton processes [14], we use an injection seeded Nd:YAG laser to provide a single mode pulse with a smooth, reproducible temporal profile having a full width at half maximum (FWHM) of 11 ns. The laser and ion beams intersect near the maximum field (0.3 T) of the permanent magnet; the divergent magnetic field adiabatically aligns and expands the photoelectron trajectories into the throat of the TOF magnetic bottle. The laser beam is tightly focused by a cylindrical lens to a 13 μm (FWHM) thick sheet perpendicular to the ion beam. The sheet height (FWHM) matches the 1 mm diameter of the ion beam. Traveling at 0.86% the speed of light, each ion transits the laser diameter in <5 ps. The photoelectron transient is time resolved by a microchannel plate (MCP) detector at the end of the 1.2 m long solenoid flight tube. A magnetic coil trims out the Earth's magnetic field transverse to the TOF tube. The signal is averaged for 1000 laser pulses using a digital oscilloscope with a time resolution of 2.5 ns. The instrument response time, limited by the laser pulse width, space charge repulsion, and nonideal magnetic collimation, is found to be approximately 20 ns by convolving Eq. (2) to fit the one-photon detached electron TOF distribution.

We examined the laser power dependence of the yield of one- and two-photon processes. The single photon

electron yield initially increases linearly with the laser irradiance and eventually saturates due to target ion depletion. The two-photon detached electron yield has a varying power law dependence that falls just below linear at the operating laser irradiance. Our rate equation model indicates that the observed power law dependence of the two-photon detachment process can be explained by the severe ion depletion due to the single photon detachment process in the high power region of the laser pulse. The predicted yield (cross sections from Ref. [18]) is overlaid on the two-photon power dependence in Fig. 2. Related studies variously attribute nonquadratic behavior to quantum interference effects from multiple detachment channels [15], incomplete overlap of the laser focus and the ion cloud [16], competition by other process [14], and partial saturation of the photodetachment probability [17]. Since our electrons are generated predominantly in a single orbital angular momentum state (as discussed below) we expect that interference is a weak effect and our sheet focus geometry assures the overlap of the ion and laser beams. We conclude that the depletion of the two-photon detachment probability due to the strong single photon absorption plays the major role in our case. We emphasize that depletion does not represent a corruption of the measurement process; in particular, it should not affect the energy or angular distribution of the one- and two-photon photoelectrons.

The angular distribution of the ejected electrons is not isotropic. Since the initial state of the ion and the final state of the neutral atom are both an S orbital, the angular momentum of the absorbed photons must be transferred to the orbital angular momentum of the ejected electron about the neutral atom. This angular momentum maps into the angular velocity distribution of the electron. In this case, as reflected in Eq. (3), the dipole selection rule for the single photon absorption requires a P wave ($\beta_2 = 2$) angular distribution in the center of mass frame, while the two-photon absorption should produce a coherent superposition between an S and a D wave distribution. The branching ratio and

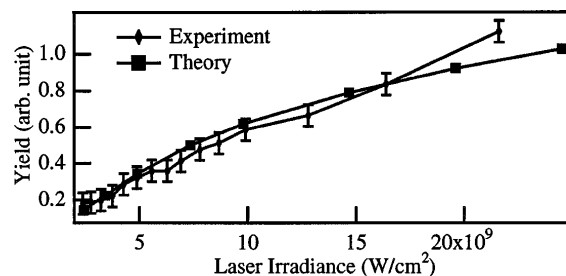


FIG. 2. Two-photon yield versus peak laser irradiance. The squares are the calculated yield using rate equations for the competing one- and two-photon processes. Cross sections were taken from Ref. [18]. The curves were normalized for best fit.

phase angle of the scattering through the S and D channels arises from the photodetachment dynamics.

In the ion rest frame, the electron distributions are monoenergetic and cylindrically symmetric about the laser polarization axis. In the laboratory rest frame, electrons ejected along the ion beam direction travel faster and arrive at the detector sooner than those ejected counter to the ion beam direction. Thus the TOF spectrum of the photodetached electrons reflects their ion center of mass angular distribution. Consequently, the β_2 and β_4 values which characterize the branching ratio and angular distribution can be inferred from the TOF spectrum taken at a particular laser polarization angle Φ . By measuring the spectrum for many values of Φ we establish the validity of our inference and reveal any systematic effects. The distribution in θ can be related to our TOF time

profile through Eqs. (2) and (3) and the relation,

$$\cos \theta = \frac{m_e d^2 / 2t^2 - (T_e + T_0)}{2\sqrt{T_e T_0}}. \quad (4)$$

We scan polarization angle, Φ , with a half-wave plate and at each angle record the TOF of the detached electrons. In Figs. 3(a) and 3(b), the lower half shows typical arrival time distributions for three values of Φ . Since the one- and two-photon arrival time distributions overlap partially, the weaker two-photon distribution is detectable only at its leading edge. Despite this masking we can still extract the anisotropy parameters in Eq. (3) by comparing different polarization angles. The leading edge of the two-photon signal is displayed in Fig. 3(b); the rising signal visible at arrival times after 380 ns marks the onset of the overlap with the strong one-photon signal. As

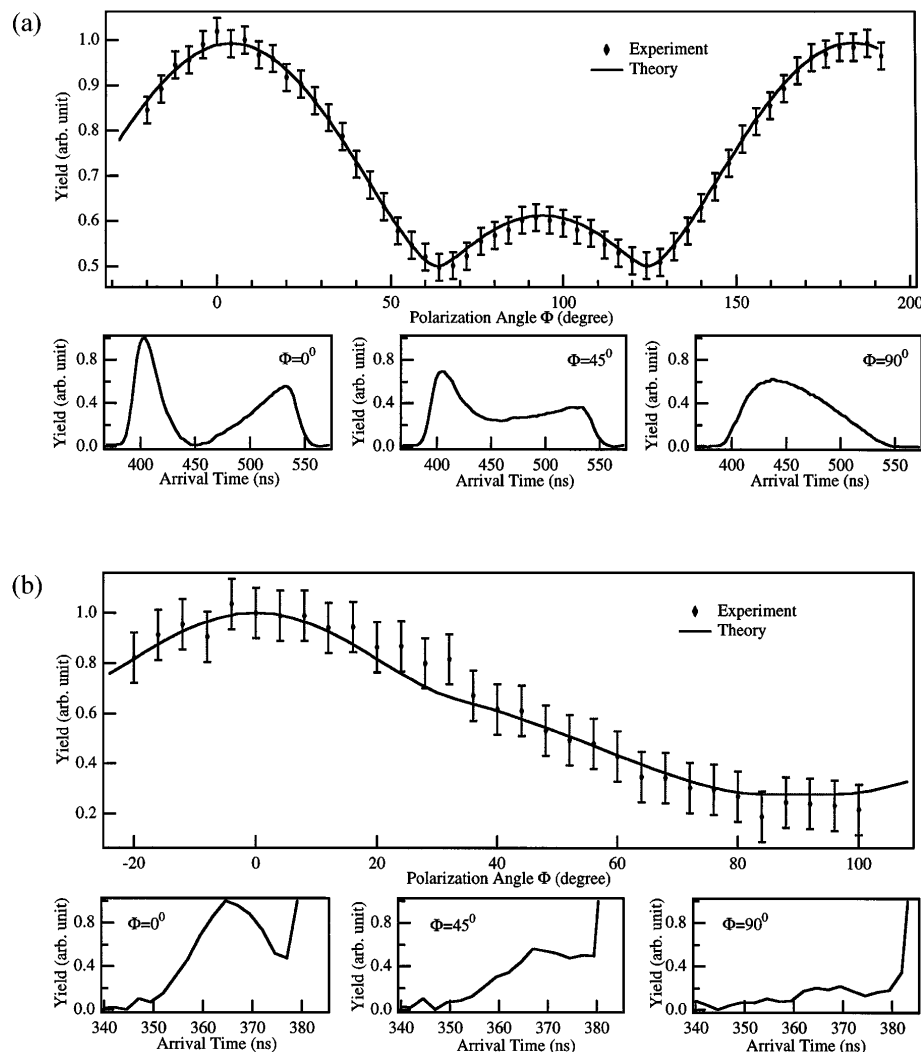


FIG. 3. Angular dependence of the TOF signal for (a) single photon and (b) two-photon detached photoelectrons. The lower plots show three typical electron arrival time distributions corresponding to three polarization angles. In the top plot, the height of the leading peak in the arrival time distribution is plotted as a function of polarization angle. The solid line (normalized to the data at 0°) is the expected behavior for a pure P and D wave angular distribution for the one- and two-photon yield, respectively. Because the two-photon data were taken with a different length flight tube there is a 2% offset in the arrival time referenced to the one photon data.

the polarization angle changes, the time profile changes in both shape and amplitude. We tabulated the height of the leading peak at each polarization angle in the top half of Figs. 3(a) and 3(b) to illustrate this amplitude variation.

The branching ratio of the S and D wave ejection processes is computed from fits to the temporal profiles. The process appears to branch at least $90\% \pm 10\%$ into the D wave. Our stated error bars depend upon the assumed phase of the S and D waves. If the relative phase angle is π , as predicted by theory (discussed below) then the fraction of S appears to be less than 10%, but if the plane wave theory is in error so that the relative phase angle is closer to zero then we cannot rule out a production of S as high as 20%. The phase angle between the S and D waves is too covariant with the branching ratio to be conclusively determined from our data. This uncertainty is due to systematic distortions of our signal inadequately accounted for in our model (most likely longitudinal space charge repulsion).

For a light atom, where the interaction of the outgoing electron with the residual core is minimal, theoretical calculations using the plane wave approximation have shown quantitative agreement with previous experiments [19]. In the plane wave approximation [20,21], the relative phases of the different angular momentum (l) amplitudes differ by $\pi\Delta l/2$, so that, in our case, the S and D wave channels should have an interference angle of π [21]. References [2,21] have shown that near threshold the fraction of population in the lower angular momentum states declines with increasing excess energy, and they report good agreement with the Wigner law [22] (which predicts that near threshold the cross section will scale as $T_e^{l+1/2}$). If the law holds far from threshold, then it predicts very little S -state production [23]. Collins and Merts [24] (momentum-space method) as well as Telnov and Chu [25] (Floquet method) predict that, at the photon energy and laser intensities in our experiment, the D state dominates in the two-photon detachment state; Telnov and Chu [25] predict greater than 90% D wave angular population. Our experimental results appear to confirm these theoretical predictions.

We have observed nonresonant excess photon detachment of the negative hydrogen ion with photons of energy greatly exceeding the binding energy. More generally, this is the first observation of nonresonant excess photon absorption in competition with the single-photon process. Even though the one-photon absorption process severely depleted the ions penetrating to the most intense region of the laser focus, we observed nonresonant EPD from a two-photon absorption. The inferred angular distribution of the electrons indicates a strong preference for a D , rather than an S , detachment channel.

The authors thank L. Collins and S.I. Chu for useful discussions, and G. Vaughn and J. Hontas for technical assistance. Authors from LANL are under Contract No. W-7405-ENG and from UNM are supported by the Division of Chemical Sciences, Office of Basic Energy Sciences, Office of Energy Research, of the U.S. Department of Energy.

-
- [1] P. Agostini, F. Fabre, G. Petite, and N.K. Rahman, Phys. Rev. Lett. **42**, 1127 (1979).
 - [2] C. Blondel, M. Crance, C. Delsart, and A. Giraud, J. Phys. B **24**, 3575 (1991).
 - [3] M.D. Davidson, H.G. Muller, and H.B. van Linden van den Heuvell, Phys. Rev. Lett. **67**, 1712 (1991).
 - [4] H. Stapelfeldt, P. Balling, C. Brink, and H.K. Haugen, Phys. Rev. Lett. **67**, 1731 (1991).
 - [5] H. Stapelfeldt and H.K. Haugen, Phys. Rev. Lett. **69**, 2638 (1992).
 - [6] A. Stintz *et al.*, Phys. Rev. Lett. **75**, 2924 (1995).
 - [7] K.R. Lykke, K.K. Murray, and W.C. Lineberger, Phys. Rev. A **43**, 6104 (1991).
 - [8] C.Y. Tang *et al.*, Phys. Rev. A **39**, 6068 (1989).
 - [9] J.T. Broad and W.P. Reinhardt, Phys. Rev. A **14**, 2159 (1976).
 - [10] H.V. Smith, J.D. Sherman, and P. Allison, Lin. Accel. Conf. Proc., CEBAF-Report-89-001, 1988, p. 164.
 - [11] H.K. Haugen, in *XVIII International Conference on the Physics of Electronic and Atomic Collisions, Aarhus, Denmark, 1993* (AIP, New York, 1993), p. 105.
 - [12] P. Kruit and F.H. Read, J. Phys. E **16**, 313 (1983).
 - [13] S.J. Smith and G. Leuchs, Adv. At. Mol. Phys. **24**, 157 (1987).
 - [14] M.R. Cervenak and N.R. Isenor, Opt. Commun. **13**, 175 (1975).
 - [15] J. Morellec, D. Normand, G. Mainfray, and C. Manus, Phys. Rev. Lett. **44**, 1394 (1980).
 - [16] R. Trainham, G.D. Fletcher, and D.J. Larson, J. Phys. B **20**, L777 (1987).
 - [17] N.B. Delone and V.P. Krainov, *Multiphoton Process in Atoms* (Springer-Verlag, New York, 1994), p. 60.
 - [18] C-R. Liu, B. Gao, and A.F. Starace, Phys. Rev. A **46**, 5985 (1992).
 - [19] M. Crance, Comments At. Mol. Phys. **24**, 95 (1990).
 - [20] M. Crance, J. Phys. B **21**, 3559 (1988).
 - [21] C. Blondel, M. Crance, C. Delsart, and A. Giraud, J. Phys. II (France) **2**, 839 (1992).
 - [22] E.P. Wigner, Phys. Rev. **73**, 1002 (1948).
 - [23] M. Crance, J. Phys. B **20**, 6553 (1987).
 - [24] L.A. Collins and A.L. Merts Phys. Rev. A **45**, 6615 (1992).
 - [25] D.A. Telnov and S.I. Chu (private communication).